a decomposition scheme similar to that described in section 4, that the back-bonding in terms of energy (ΔE_{B_2}) is more important than the donation (ΔE_{A_1}) for the stability of $Ni(PH_3)_2(C_2H_2)$ and $Ni(PH_3)_2(C_2H_4)$. The calculated bonding energies were somewhat smaller than those obtained in the present work, 126 kJ mol^{-1} for $Ni(PH_3)_2(C_2H_4)$ and 154 kJ mol^{-1} for $Ni(PH_3)_2(C_2H_2)$.

Experimental bonding energies are not available for a homologous series of $ML_n(C_2H_2)$ or $ML_n(C_2H_4)$ complexes in which M is varied along a triad. It is however assumed, on the basis of experimental equilibrium constants for olefin and acetylene addition, that the stability order, in agreement with our findings, is 3d > 5d > 4d. For alkenes and alkynes complexed to $M(PR_3)_2$ bonding energies have only been determined for a few olefin complexes of $Ni(PR_3)_2$, via the reaction

$$Ni(PR_3)_4 + C_2H_4 = Ni(PR_3)_2(C_2H_4) + 2PR_3 \quad (5.1)$$

The determination of the bonding energy from eq 5.1 is however somewhat hampered by the lack of accurate values for the energy required to dissociate two PR_3 ligands from $Ni(PR_3)_4$. Tolman et al.[4c] give in their latest estimate a bonding energy of 167 kJ mol^{-1} for $Ni(P(O\text{-}p\text{-tolyl})_3)_2(C_2H_4)$. The good agreement between this value and a calculated bonding energy of 166.9 kJ mol^{-1} for $Ni(PH_3)_2(C_2H_4)$ (Table III) is clearly fortuitous. One wouuld in fact expect the bonding energy of $Ni(PH_3)_2(C_2H_4)$ to be larger than the bonding energy of $Ni(P(O\text{-}p\text{-tolyl})_3)_2(C_2H_4)$, since the deformation of $Ni(PR_3)_2$ from **1** to **2** on steric grounds must require more energy for R = O-*p*-tolyl than for R = H. The bonding energy for alkenes and alkynes complexed to $M(PR_3)_4^+$ can be determined directly via the process

$$M(PR_3)_4^+ + XY = M(PR_3)_4(XY)^+ \quad (5.2)$$

For $Ir(PPh_3)_2(CO)Cl$ the bonding energies with C_2H_4 and C_2H_2 were determined[4a] in solution to be 49.4 and 38.9 kJ mol^{-1}, respectively. Data from analogous complexes of Co and Rh are not available.

We have calculated the $M(PH_3)_2$ fragments to form stronger π complexes with C_2H_2 and C_2H_4 than the $M(PH_3)_4^+$ fragments in spite of the larger contribution from ΔE_{A_1} to the stability of $M(PH_3)_4(C_2H_2)^+$ and $M(PH_3)_4(C_2H_4)^+$. The difference in stability can, just as for the dioxygen complexes, be traced to ΔE_{prep} and the substantial energy required to deform $M(PH_3)_4^+$ from conformation **3** to conformation **4**. It should however be pointed out that d^{10} complexes of Ni, Pd, and Pt with phosphine ligands exist as $M(PR_3)_4$ or $M(PR_3)_3$ species rather than in the coordinatively unsaturated form $M(PR_3)_2$. The formation of the d^{10} complex $M(PR_3)_2XY$ will as a consequence require the dissociation of one or two PR_3 ligands (see eq 5.1), and $M(PR_3)_2(XY)$ might for this reason not be more readily formed than $M(PR_3)_4(XY)^+$.

6. Concluding Remarks

Our approach is approximae, aside from the inherent limitations of the HFS method, since we have been forced of necessity to represent the ML_2 and ML_4 fragments by $M(PH_3)_2$ or $M(PH_3)_4^+$ model systems using standard structural parameters rather than optimized geometries. It has however been possible within such limitations to carry out a systematic study of unsaturated ligands such as O_2, C_2H_2, and C_2H_4, complexed to d^{10} ML_2 fragments as well as d^8 ML_4 fragments.

Our calculations indicate that d^{10} ML_2 fragments as well as d^8 ML_4 fragments of 3d elements form stronger π complexes with the unsaturated ligands O_2, C_2H_2, and C_2H_4 than the corresponding ML_n fragments of the 4d and 5d elements, and we have given in section 4 a possible rationale for this trend.

We have further found, on the basis of an energy decomposition analysis, that the back-donation in the Dewar–Chatt–Duncanson model in terms of energy is more important for the stability of the systems discussed here than the donation. It has also been demonstrated that the ML_4 fragments are less prone to form π complexes than the ML_2 fragments, as a substantial energy is required to deform the pseudo-square-planar conformation **3** of ML_4 in the free state to the butterfly geometry **4** adopted in the $ML_4(XY)$ complexes.

Our calculations indicate finally that the bonding energies in an analogous set of complexes with O_2, C_2H_2, and C_2H_4 follow the order $O_2 > C_2H_2 \sim C_2H_4$.

Acknowledgment. This investigation was supported by the Natural Sciences and Engineering Research Council of Canada (NSERC).

Contribution from the Department of Chemistry,
Monash University, Clayton, Victoria 3168, Australia

Magnetic Properties and Zero-Field Splitting in High-Spin Manganese(III) Complexes. 1. Mononuclear and Polynuclear Schiff-Base Chelates

BRENDAN J. KENNEDY and KEITH S. MURRAY*

Received June 11, 1984

Variable-temperature (4.2–300 K) and variable-field (4.2 K, 5–50 kG) susceptibility measurements have been made on a range of manganese(III) Schiff-base complexes. The compounds studied contain either tetradentate salicylaldimines and β-ketone imines of the types [Mn(salen)X] and [Mn(acen)X], where X is Cl$^-$, Br$^-$, OAc$^-$, SCN$^-$, N_3^-, or bidentate salicylaldimines of the type $Mn(sal\text{-}NR)_3$. The measurements were generally made on Vaseline mulls of the samples in order to avoid anomalous results due to crystallite alignment. Spin Hamiltonian theory has been used to deduce values of the zero-field splitting parameter, *D*, and the exchange coupling parameter, *J*. The *D* values fall in the range −1 to −4 cm^{-1}. *J* values of less than −1 cm^{-1} were detected in some of the "monomers" and up to −5.4 cm^{-1} in the dimer or linear-chain examples. In linear chains such as [Mn(salen)OAc] and [Mn(salen)N_3] a small interchain exchange contribution was required to completely explain the data.

Introduction

High-spin manganese(III) complexes have a ^5D ground term that is split in octahedral crystal fields to produce $^5T_{2g}$ and ^5E_g terms. The effect of noncubic symmetry and/or Jahn–Teller distortions is to remove the oribtal degeneracy of the ^5E_g ground term to give an orbital singlet lowest, either a $^5A_{1g}$ or $^5B_{1g}$ (in D_{4h} symmetry). The spin degeneracy of the ground state is further removed by spin–orbit coupling, giving rise to the so-called

0020-1669/85/1324-1552$01.50/0

zero-field splitting[1] (ZFS).

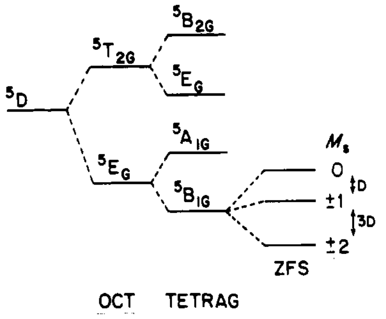

The exact nature of the ground state depends critically on the symmetry of the ligand field about the metal ion. If the $d_{x^2-y^2}$ orbital is unoccupied, then the complex is expected to be axially elongated, with the $^5B_{1g}$ level lying lowest. Such a ground term is expected[2] to have principal susceptibilities in the order $K_\parallel > K_\perp$, and hence D will be negative. Conversely, compression of the octahedron results in the $^5A_{1g}$ lying lowest with D positive.

The zero-field splitting in Mn(III) is typically of the order of a few wavenumbers, and so the magnetic properties are expected to be Curie-like and close to spin only (4.90 μ_B), except at very low temperatures where a rapid decrease in μ_{Mn} occurs.

A number of early studies[3-6] on five- and six-coordinate Mn(III) Schiff-base complexes showed that these complexes displayed Curie-like behavior in the temperature range 80–300 K with magnetic moments of about 4.9 μ_B. Owing to the small size of the ZFS, together with the possibilities of weak magnetic exchange, exact interpretation of the data was not always possible, and the possibility of relatively large errors in the magnitude of such interactions existed.

More recently, a number of structural studies on Mn(III) Schiff-base complexes have been reported,[7-10] often showing the presence of quite appreciable distortions about the Mn(III) center. It seemed desirable to examine the magnetic properties of some of these types of complexes in more detail, utilizing a wider range of temperatures and magnetic fields than previously employed. In this way it should be possible to quantify the nature and strength of any magnetic exchange interactions and/or zero-field splittings. In the present paper the results of our magnetic studies on some monomeric and polymeric Schiff-base complexes of the types [Mn(bidentate)$_3$] and [Mn(tetradentate)X] are described. Where possible, the results are discussed in terms of their molecular structures.

Experimental Section

Materials and Synthesis. [Mn(sal-*N*-Benz)$_3$], [Mn(sal-*N*-Ph)$_3$], [Mn(salen)Br], and [Mn(salen)OAc] were prepared and characterized as described elsewhere.[3]

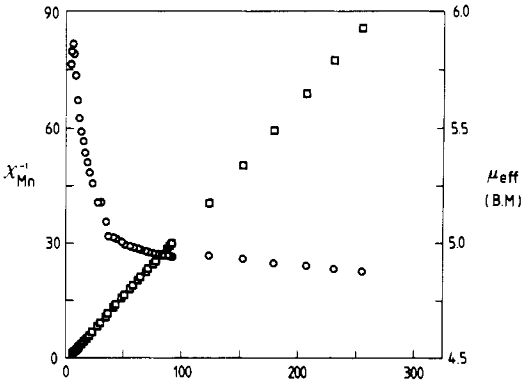

Figure 1. Temperature dependence of the magnetic moment (○) and reciprocal susceptibility (□) for a polycrystalline sample of [Mn(sal-*N*-Ph)$_3$] (H = 10000 G).

[Mn(acac)$_2$SCN] and [Mn(acac)$_2$N$_3$] were prepared by the method of Stults et al.[11,12] [Mn(acen)Cl] and [Mn(acen)N$_3$] were prepared by a modified method of Boucher and Day.[9] Multiple extractions with chloroform were found to be necessary in order to obtain a reasonable yield of the complex. The complexes were characterized by microanalysis, IR spectra, and melting points.

[Mn(salen)SCN]. Equimolar amounts of [Mn(acac)$_2$SCN] and salenH$_2$ were refluxed in 20 mL of a 1:3 solution of DMF/ethanol for 30 min. The solution was then slowly cooled and the resulting black/green precipitate collected, washed with cold ethanol, and dried in vacuo over P$_2$O$_5$ for 12 h. IR: ν_{SCN} 2050, 775 cm^{-1}. Anal. Calcd for $C_{17}H_{14}MnN_3O_2S$: C, 53.84; H, 3.72; N, 11.02. Found: C, 54.00; H, 3.67; N, 11.15. **[Mn(salen)N$_3$]** was prepared from [Mn(acac)$_2$N$_3$] in a manner similar to that above, but with some modifications. After the solution was refluxed for 10 min, the mixture was rapidly cooled in an ice bath and the fine yellow precipitate collected, washed with dry ether, and dried in vacuo over P$_2$O$_5$ for 24 h. This complex appears to be slightly hygroscopic and was stored over P$_2$O$_5$. IR: ν_{N_3} 2040 cm^{-1}. Anal. Calcd for $C_{16}H_{14}MnN_5O_2$: C, 52.91; H, 3.89; N, 19.28. Found: C, 52.52; H, 3.60; N, 19.69.

[Mn(salen)NO$_2$]. Mn(salen)Br (0.5 g) was dissolved in a minimum amount of cold ethanol and a saturated aqueous solution of NaNO$_2$ added. The resulting solution was stirred for 12 h and the dark precipitate collected. The crude solid was then recrystallized from dry ethanol, filtered, washed with dry ether, and finally dried in vacuo over P$_2$O$_5$ for 12 h. IR: ν_{NO_2} 1200, 1040 cm^{-1}. Anal. Calcd for $C_{16}H_{14}MnN_3O_4$: C, 52.33; H, 3.84; N, 11.44. Found: C, 52.16; H, 3.84; N, 11.64.

Physical Measurements. Average magnetic susceptibilities were measured on an extensively modified Oxford Instruments magnetometer.[13] Samples were run as neat powders between 4.2 and 300 K with a main field of 10 kG and a gradient field of 1000 G/cm. Measurements were made manually between 4.2 and 20 K, with automatic data logging equipment used at higher temperatures. Temperatures below 30 K were measured on a carbon resistor while above this a Cu/constantan thermocouple was employed. The carbon resistor was found to be slightly field dependent below ca. 10 K. For measurements at other than the lowest attainable temperature (ca. 4.28 K) errors of up to 0.2 K can result from this effect. In general, the errors in temperature were found to be less than 0.1 K.

Magnetization measurements at seven field strengths between 5 and 50 kG were made at several temperatures between 4.2 and 20 K. Due to the tendency of some samples to align in high magnetic fields and low temperatures, samples were ground with Vaseline and a uniform mull was prepared. Measurements were made with both increasing and decreasing magnetic fields, and there was no evidence of sample orientation.

The mass of the sample contained within the Vaseline mulls was determined by comparing the gram susceptibility of the neat powder at 10 kG with that of the mull, once corrections for the diamagnetic sample holder and Vaseline had been made, over a temperature range of not less than 30 K. In general, for six to ten overlapping points the mass could be estimated to bettern than 0.1% for a 20-mg sample.

All samples used for variable-temperature susceptibility studies were found to give field-independent susceptibilities at room temperature.

Results and Discussion

(i) Monomers. The plot of reciprocal susceptibilities against temperature for a finely ground powder sample of [Mn(sal-*N*-

---

(1) A comprehensive set of calculations of the susceptibilities and magnetizations for Mn(III) ions has been carried out by using spin Hamiltonian and matrix diagonalization techniques under axial and rhombic symmetries in both the presence and absence of weak exchange coupling. The results, presented in graphical form, together with tables of matrix elements, are available on request to the authors.

(2) Mitra, S. *Prog. Inorg. Chem.* **1977**, *22*, 309.

(3) van den Bergen, A.; Murray, K. S.; O'Connor, M. J.; West, B. O. *Aust. J. Chem.* **1969**, *22*, 39.

(4) Lewis, J.; Mabbs, F. E.; Weigold, H. *J. Chem. Soc. A* **1968**, 1699.

(5) Earnshaw, A.; King, E. A.; Larkworthy, L. F. *J. Chem. Soc. A* **1968**, 1048.

(6) Zelentsov, V. V.; Somova, I. K. *Russ. J. Inorg. Chem.* (*Engl. Transl.*) **1973**, *18*, 1125.

(7) Davies, J. E.; Gatehouse, B. M.; Murray, K. S. *J. Chem. Soc. Dalton Trans.* **1973**, 2523.

(8) Raston, C. L.; White, A. L.; Willis, A. C.; Murray, K. S. *J. Chem. Soc., Dalton Trans.* **1974**, 1793.

(9) Boucher, L. J.; Day, V. W. *Inorg. Chem.* **1977**, *16*, 1360.

(10) Mikuriya, M.; Torikara, N.; Okawa, H.; Kida, S. *Bull. Chem. Soc. Jpn.* **1981**, *54*, 1063.

(11) Stults, B. R.; Day, R. O.; Marianelli, R. S.; Day, V. W. *Inorg. Chem.* **1979**, *18*, 1847.

(12) Stults, B. R.; Marianelli, R. S.; Day, V. W. *Inorg. Chem.* **1975**, *14*, 722.

(13) Mackey, D. J.; Evans, S. V.; Martin, R. L. *J. Chem. Soc., Dalton Trans.* **1976**, 1515.

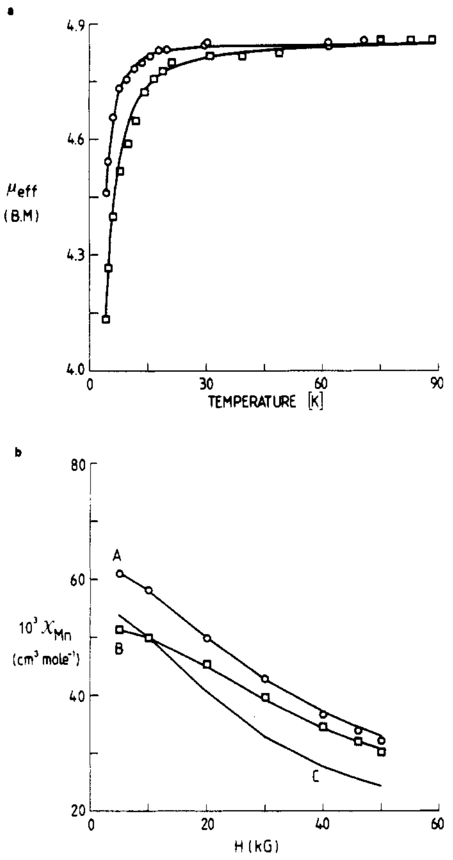

Figure 2. (a) Average magnetic moment of [Mn(sal-*N*-Ph)$_3$] (○) and [Mn(sal-*N*-Benz)$_3$] (□) for Vaseline-mulled samples. The solid line for [Mn(sal-*N*-Ph)$_3$] is for $D = -2.1$ cm^{-1} and $g = 1.99$, and for [Mn(sal-*N*-Benz)$_3$] the line is compatible for both $D = -2.6$ cm^{-1} and $g = 1.99$ ($J = -0.08$ cm^{-1}) and $D = -4.9$ cm^{-1} and $g = 1.99$ (see text) ($H = 10000$ G). (b) Magnetization of [Mn(sal-*N*-Ph)$_3$] (○) and [Mn(sal-*N*-Benz)$_3$] (□) at 4.2 K for Vaseline-mulled samples. Solid lines are calculated as described in text. (NB: Near the saturation limit, plots of susceptibility are not strictly correct. A better quantity is the reduced moment $\langle\mu\rangle$ used in Figure 3b. It is instructive, however, to see how χ varies as a function of H.) Conditions: (A) $D = -2.1$ cm^{-1}, $g = 1.99$; (B) $D = -2.6$ cm^{-1}, $g = 1.99$, $J = -0.08$ cm^{-1}; (C) $D = -4.9$ cm^{-1}, $g = 1.99$.

Ph)$_3$] obtained at 10 kG appears Curie-like ($\Theta = -2.7$ K, C 0.338) (Figure 1). However, the corresponding magnetic moments show a very rapid and unexpected increase in μ_{eff} below ca. 25 K, reaching a maximum of 5.9 μ_B at ca. 6 K before decreasing again. [Mn(sal-*N*-Benz)$_3$] behaves in a similar manner. This behavior is similar to that calculated for μ in a single crystal when D is negative[2] and is thought to arise from the powder sample acting as an oriented single crystal owing to large magnetic anisotropy and/or alignment in the magnetic field. Similar behavior has recently been reported for a number of high-spin Fe(II)[14] chelate complexes in which D is negative and has also been observed in high-spin Fe(III) porphyrin complexes in which D is positive.[15]

Grinding of [Mn(sal-*N*-Ph)$_3$] with Vaseline results in a slight lowering of μ_{eff} at all temperatures, such that μ_{eff} remains constant at 4.86 μ_B down to ca. 20 K below which it drops quite rapidly to 4.5 μ_B at 4.2 K (Figure 2). This behavior is that expected for a high-spin Mn(III) complex in which there is appreciable zero-field splitting of the ground state and/or weak antiferromagnetic coupling. The magnetic behavior of [Mn(sal-*N*-Benz)$_3$] ground with Vaseline is very similar (Figure 2), with μ_{eff} remaining constant at 4.87 μ_B above ca. 30 K, while below this it rapidly decreases to 4.14 μ_B at 4.2 K, suggesting that slightly larger zero-field splitting and/or antiferromagnetic coupling is present compared to the phenyl complex. The published[8] crystal structure of [Mn(sal-*N*-Benz)$_3$] shows the Mn(III) center to exist in a distorted octahedral arrangement as a result of Jahn–Teller effects. This results in four short and two long Mn–L bond lengths that correspond to a $^5B_{1g}$ ground state, where D is negative and the $M_S = \pm 2$ Kramer's doublet is lowest.[16,17]

Preliminary fits to the observed data were obtained by using the spin Hamiltonian (1) in which any rhombic splitting was

$$\mathcal{H} = g\beta\hat{H}\cdot\hat{S} + D[\hat{S}_z^2 - \tfrac{1}{3}S(S + 1)] \qquad (1)$$

ignored. Computer diagonalization of the resultant matrix and use of a spatial averaging technique[18,19] together with the experimental magnetic field of 10 kG, to calculate susceptibilities, gave a best fit for [Mn(sal-*N*-Benz)$_3$] of $g = 1.99$ and $D = \pm 4.9$ cm^{-1} and for [Mn(sal-*N*-Ph)$_3$] of $g = 1.99$ and $D = \pm 2.1$ cm^{-1}. As has been observed previously,[1,20] the powder susceptibility data were not sensitive to the sign of the ZFS although the magnitude could readily be estimated. Although the structural data for [Mn(sal-*N*-Benz)$_3$] strongly support a $^5B_{1g}$ ground state, and hence negative D, it was thought the measurements over a range of magnetic fields would be capable of confirming the sign of D for this complex as well as resolving the sign of D for the related phenyl complex. As can be seen from Figure 2b, it is possible to explain the field dependence of susceptibilities for [Mn(sal-*N*-Ph)$_3$] at 4.2 K in terms of the Hamiltonian described above with $D = -2.1 \pm 0.1$ cm^{-1}. The fit was noticeably worse when positive values of D were employed. The situation was found to be more complex for [Mn(sal-*N*-Benz)$_3$], with only moderate fits being observed for D equal to ± 4.9 cm^{-1}. An acceptable fit at fields above 30 kG could be obtained with $D = -2.5$ cm^{-1}.

However, no one value of D, either positive or negative, could reproduce the observed data at all fields. Examination of the structure at this complex indicated that the symmetry was probably less than axial, and so a rhombic term was added to the Hamiltonian. Although such a term resulted in a marginally better fit to the temperature susceptibility data, it was still not possible to fit the magnetization data to unique values of D and E.

As discussed previously,[1,21] weak antiferromagnetic coupling has a similar effect to ZFS on the low-temperature magnetic susceptibilities. It does not, however, cause a similar field-dependent behavior at very low temperatures. The possibility of weak magnetic exchange in Mn(sal-*N*-Benz)$_3$ was, therefore, considered, assuming a pairwise interaction between two zero-field split Mn(III) ions such that the spin Hamiltonian becomes

$$\mathcal{H} = g_1\beta\hat{H}\cdot\hat{S}_1 + g_2\beta\hat{H}\cdot\hat{S}_2 - 2J\hat{S}_1\hat{S}_2 + D_1[\hat{S}_{1z}^2 - \tfrac{1}{3}S_1(S_1 + 1)] + D_2[\hat{S}_{2z}^2 - \tfrac{1}{3}S_2(S_2 + 1)] \qquad (2)$$

To reduce the number of variables, it was then assumed that $g_1 = g_2$ and $D_1 = D_2$, i.e. a symmetrical dimer. Careful and systematic variation of g, D, and J gave best fit parameters of $g = 1.99 \pm 0.01$, $D = -2.6 \pm 0.1$ cm^{-1}, and $J = -0.08 \pm 0.01$ cm^{-1}, which as seen in Figure 2b adequately reproduce both the temperature and field dependence of the susceptibilities.

The structural data[8] for [Me(sal-*N*-Benz)$_3$] show no obvious pathway for the magnetic exchange. We note, however, that Gregson[22] has reported similar problems in explaining the magnetic behavior of Mo(acac)$_3$, a complex in which exchange interactions were also important and in which no obvious exchange pathway existed.[23] However, when considering the very small size of the exchange, -0.08 cm^{-1}, the absence of an obvious pathway is perhaps not surprising.

The crystal structure of [Mn(acen)Cl] shows[9] it to exist as discrete monomeric units with a distorted square-pyramidal ge-

---

(14) Reiff, W. M.; Nicolini, C.; Dockum, B. *J. Phys. Coll.* **1979**, *40*, C2-230.
(15) Behere, D. V.; Date, S. K.; Mitra, S. *Chem. Phys. Lett.* **1979**, *68*, 544.
(16) Gerritsen, H. J.; Sabinsky, E. S. *Phys. Rev.* **1963**, *132*, 1507.
(17) Mathe, J.; Schinkel, C. J.; van Amstel, W. A. *Chem. Phys. Lett.* **1975**, *33*, 528.
(18) Marathe, V. R.; Mitra, S. *Chem. Phys. Lett.* **1974**, *27*, 103.
(19) Vermaas, A.; Groenveld, W. L. *Chem. Phys. Lett.* **1974**, *27*, 583.
(20) Behere, D. V.; Mitra, S. *Inorg. Chem.* **1980**, *19*, 992.
(21) Behere, D. V.; Marathe, V. R.; Mitra, S. *Chem. Phys. Lett.* **1981**, *81*, 57.
(22) Gregson, A. K.; Anker, M. *Aust. J. Chem.* **1979**, *32*, 503.
(23) Raston, C. L.; White, A. H. *Aust. J. Chem.* **1979**, *32*, 507.

Table I

compd	μ_{eff} (295 K), μ_B	D, cm^{-1}	J, cm^{-1}	ZJ', cm^{-1}	g	model
[Mn(sal-*N*-Ph)$_3$]	4.87	−2.1 ± 0.1	0	0	1.99 ± 0.01	1
[Mn(sal-*N*-Benz)$_3$]	4.86	−2.6 ± 0.1	−0.08 ± 0.01	0	1.99 ± 0.01	2
[Mn(acen)Cl]	4.91	−1.6 ± 0.1	−0.10 ± 0.01	0	2.00 ± 0.01	2
[Mn(salen)SCN]	4.88	−3.8 ± 0.2	−0.44 ± 0.02	0	1.97 ± 0.02	2
[Mn(salen)Br]	4.75	−1.0 ± 0.3	−1.84 ± 0.10	0	1.95 ± 0.03	2
[Mn(salen)OAc]	4.74	0	−1.8	0.10	1.98 ± 0.01	3/4
		0	−1.5 ± 0.1	1.00 ± 0.05	1.98 ± 0.01	5/4
[Mn(salen)N$_3$]	4.53	0	−5.42 ± 0.10	−0.18 ± 0.05	1.98 ± 0.01	3/4
		0	−4.45 ± 0.05	−1.4 ± 0.2	1.98 ± 0.01	5/4
[Mn(acen)N$_3$]	4.68	0	−2.92 ± 0.05	0 ± 0.10	2.00 ± 0.02	3/4
		0	−2.73 ± 0.05	0 ± 0.10	2.00 ± 0.02	5/4

ometry around Mn. The magnetic moment shows a similar temperature dependence to the six-coordinate complexes (Figure 3a) and can be explained by using the axial spin Hamiltonian with $|D| = 3$ cm^{-1}. It was not possible to obtain an estimate of the size of E from these data when a rhombic Hamiltonian was used. Surprisingly, it was not possible to explain the results of detailed magnetization measurements over the temperature range 4–20 K with either an axial or rhombic spin Hamiltonian. However, use of a dimeric model indicated that exchange coupling was occurring, and a least-squares fitting of the results yielded best fit parameters of $g = 2.00 \pm 0.01$, $D = -1.6 \pm 0.1$ cm^{-1}, and $J = -0.10 \pm 0.01$ cm^{-1}. The sign and size of D deduced here are comparable to those reported by Mitra et al.[21] for the related porphyrin complex Mn(TPP)Cl, where weak exchange coupling was also detected. Although not obvious from the published structural data, the chloride ion is probably involved in the exchange pathway, in a similar way to that recently discussed by Murray et al. for a chloroiron(III) thiohydroxamate complex.[24]

Powder samples of [Mn(salen)NO$_2$] exhibit behavior similar to that shown in Figure 1. This complex was originally studied in order to examine magnetic exchange effects via a bridging nitrito group. Close examination of the data showed alignment of the sample occurring in the presence of magnetic fields, even for applied fields as low as 5 kG (our lowest stable field). This behavior suggests that for this complex D is also negative and that magnetic exchange is very weak, since for all polymeric species studied there was no evidence for alignment in the magnetic field. It appears that this behavior is a result of having the magnetic Kramer's doublet $M_S = \pm 2$ lowest, although, as noted earlier, there are examples of Fe(III) complexes with positive D values that show alignment.[15]

The above results demonstrate the usefulness of magnetization measurements in determining both the size and sign of zero-field splittings. In addition, such measurements enable very weak exchange interactions to be identified. If exchange interactions are not considered, a marked overestimation of the size of any ZFS could result.

(ii) Chains. Three of the complexes studied, namely [Mn(salen)OAc], [Mn(salen)N$_3$], and [Mn(acen)N$_3$], show a broad maximum in susceptibility at low temperatures, which is indicative of antiferromagnetic coupling within a chain-type structure. For each of these complexes the room-temperature magnetic moments are slightly reduced below the spin-only value of 4.9 μ_B (Table I).

The structure of [Mn(salen)OAc] has been reported[7] and consists of linear chains of approximately planar Mn(salen) moieties bridged by a single acetate group in an anti–anti configuration. Like [Mn(sal-*N*-Benz)$_3$], the manganese atom in [Mn(salen)OAc] exists in a distorted octahedral arrangement, with the Mn–O(acetate) bond length of 2.201 Å being considerably longer than the Mn–O(phenol) distance of 1.888 Å. This results in a {two long, four short} distortion corresponding to the $^5B_{1g}$ ground state. Several attempts to grow crystals of the azide complex suitable for diffraction studies were unsuccessful.

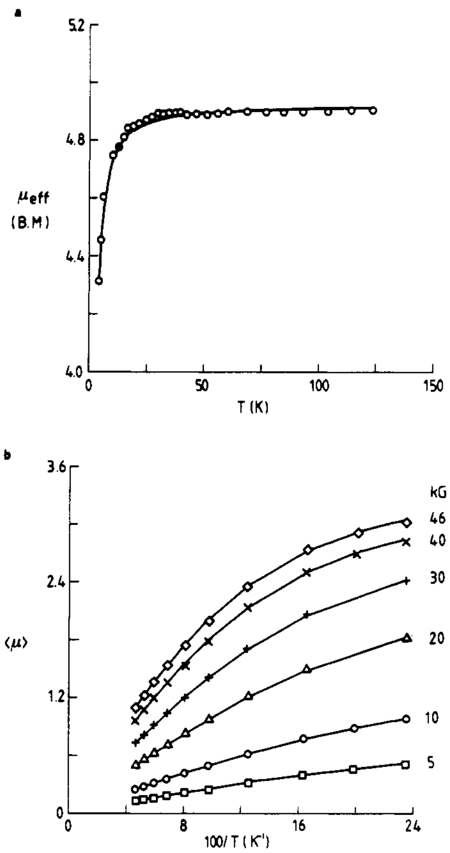

Figure 3. (a) Average magnetic moment of [Mn(acen)Cl] at 10 kG. Solid lines is for $D = -1.6$ cm^{-1}, $J = -0.10$ cm^{-1}, and $g = 2.00$. (b) Magnetization data for [Mn(acen)Cl] between 4 and 20 K. The solid lines are for $D = -1.6$ cm^{-1}, $J = -0.10$ cm^{-1}, and $g = 2.00$ ($\langle\mu\rangle = \chi H/N\beta$).

In general, Mn(III) is expected to be Heisenberg-like in its behavior, except at very low temperatures where some anisotropy may be important. Attempts were, therefore, made to explain the magnetic behavior in terms of the Heisenberg one-dimensional chain, using expression 3 derived by Fisher,[25] where by definition

$$\chi = \frac{N\beta^2 g^2}{3kT} S(S+1)\left[\frac{1+U}{1-U}\right] \tag{3}$$

$$U = \coth \frac{-2JS(S+1)}{kT} - \frac{2JS(S+1)}{kT}$$

a positive J corresponds to *antiferromagnetic* coupling. (A uniform convention for the sign of J has been used in the text and in Table I; viz. negative J corresponding to antiferromagnetism.) Least-squares fitting of the observed data for [Mn(salen)OAc] to (3) gave best fit parameters of $g = 1.98$ and $J = -1.54$ cm^{-1} in reasonable agreement with those deduced by Davies et al.[7] on the

---

(24) Berry, K. J.; Clark, P. E.; Murray, K. S.; Raston, C. L.; White, A. H. *Inorg. Chem.* **1983**, *22*, 3928.

(25) Wagner, G. R.; Friedberg, S. A. *Phys. Lett.* **1964**, *9*, 11.

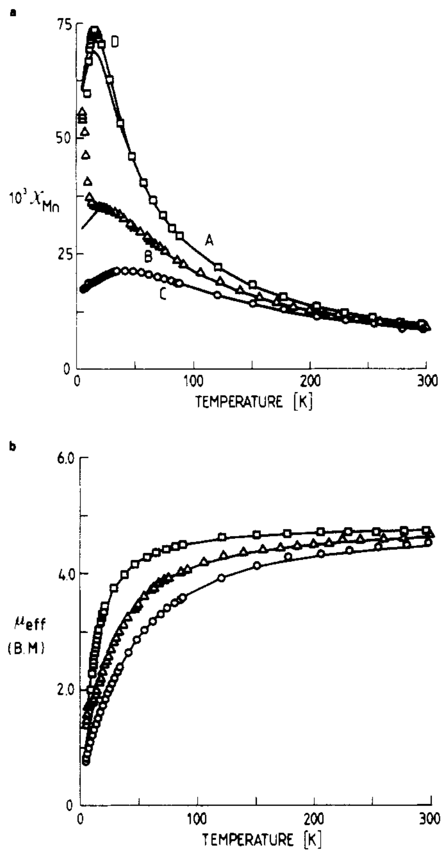

Figure 4. (a) Magnetic susceptibility plots for [Mn(salen)OAc] (□), [Mn(salen)N_3] (○), and [Mn(acen)N_3] (△). Solid-line data for eq 3: (A) $J = -1.8$ cm^{-1}, $ZJ' = 0.10$ cm^{-1}, $g = 1.98$; (B) $J = -2.92$ cm^{-1}, $ZJ' = -0.18$ cm^{-1}, $g = 1.98$; (C) $J = -5.42$ cm^{-1}, $ZJ' = 0$ cm^{-1}, $g = 2.00$. Solid-line data for eq 5: (D) $J = -1.5$ cm^{-1}, $ZJ' = 1.00$ cm^{-1}, $g = 1.98$. (b) Average magnetic moments of [Mn(salen)OAc] (□), [Mn(salen)N_3] (○), and [Mn(acen)N_3] (△). Solid lines are calculated as above.

basis of data measured between 80 and 300 K. The R factor found, 4.5%, was however rather large. The goodness of fit factor R is defined as

$$\frac{\sum_o^i [\chi_i^{\text{calcd}} - \chi_i^{\text{obsd}}) T_i}{\sum \chi_i^{\text{obsd}} T_i}$$

In order to improve on this, eq 3 was then modified to include interchain effects[25] so that

$$\chi' = \chi/[1 - (2ZJ'/Ng^2\beta^2)\chi] \qquad (4)$$

where χ' is the corrected susceptibility, Z the number of nearest neighbor, and J' the exchange integral for the magnetic interaction between nearest-neighbor chains. The addition of this extra term led to a marked improvement in the fit, with R dropping to 2.35% for the parameters given in Table I. Nevertheless, as seen from Figure 4a, the agreement between observed and calculated susceptibilities around 20 K is poor, which suggests that an additional effect may be present.

An alternative expression (5) for an $S = 2$ chain, based on Weng's numerical results,[26] has been reported recently by Hatfield

$$\chi = \frac{N\beta^2 g^2}{kT}\left[\frac{A + Bx^2}{1 + Cx + Dx^3}\right] \qquad (5)$$

and co-workers,[27] where $A = 2.0000$, $B = 71.938$, $C = 10.482$, $D = 955.56$, and $X = |J|/kT$. This expression may be modified to include interchain effects in a manner similar to that given above.

Least-squares fitting of the results to (5) lead to best fit parameters of $g = 1.98 \pm 0.01$, $J = -1.5 \pm 0.1$, and $ZJ' = 1.00 \pm 0.05$ cm^{-1}, where a relatively large ferromagnetic interchain interaction is present. As seen from Figure 4, these parameters reproduce the observed susceptibilities very well ($R = 1.78\%$) except at very low temperatures where the effects of ZFS and a small amount of uncoupled species appear important.

Davies et al.[7] concluded from their structural study on [Mn(salen)OAc] that interchain interactions were expected to be negligible, and it is possible that this apparent large interaction arises from another effect. As the $M_S = \pm 2$ Kramer's doublet lies lowest in the present complex, the possibility of three-dimensional magnetic ordering exists. Gregson and Moxon[28] have recently observed ferromagnetic canting of the spins in the related complexes [Mn(acac)$_2$X] (X = SCN, N_3), which have a similar ground state. This may also provide the explanation for the unusual behavior observed here. It should be stressed that the magnetic ordering in the present case and in those studied by Gregson and Moxon[28] is different from that observed for the monomeric complex discussed in section i where alignment of the sample crystallites in the magnetic field is responsible for the increased susceptibilities.

The magnetic properties of [Mn(salen)N_3] are generally similar to those of [Mn(salen)OAc], with the maximum in susceptibility at the azide complex occurring at a slightly higher temperature, indicating stronger magnetic exchange. Application of the modified Fisher expression led to best fit parameters of $g = 1.98 \pm 0.01$, $J = -5.42 \pm 0.10$ cm^{-1}, and $ZJ' = -0.18 \pm 0.05$ cm^{-1}. In this case, weak antiferromagnetic interchain interactions are present. Use of Hatfield's expression[27] led to a fit of similar quality and $g = 1.98 \pm 0.01$ and $J = -4.45 \pm 0.05$ cm^{-1} with $ZJ' = -1.4 \pm 0.2$ cm^{-1}. The interchain interaction is calculated to be slightly stronger than in the acetate complex. If it is assumed that $ZJ' = 0$, then the values of $J = -5.0 \pm 0.1$ cm^{-1} (Fisher model) and -4.5 ± 0.2 cm^{-1} (Hatfield model) obtained are reasonably similar.

[Mn(acen)N_3] shows magnetic properties in the temperature range 20–300 K that can be explained in terms of an $S = 2$ Heisenberg chain. Both models gave almost identical fits; viz., $g = 2.00 \pm 0.02$ and $J = -2.8 \pm 0.1$ cm^{-1}. Below 20 K the susceptibilities remain reasonably constant down to 10 K, below which they increase very rapidly (Figure 4). This low-temperature behavior may be a result of either some uncoupled Mn(III) species being present or of ferromagnetic canting of the spins. It was not possible to reproduce the susceptibilities from an additive relationship of the type $\chi_{\text{obsd}} = A\chi_{\text{monomer}} + (1-A)\chi_{\text{chain}}$ where χ_{monomer} was calculated for a zero-field split monomer by using eq 1 and χ_{chain} was calculated from eq 3. This would suggest that a monomer impurity is not the reason for the rapid increase in susceptibility. This observation, together with the anomalously large field dependence found at 4.2 K, suggests that long-range ordering is also important in this complex. The related complex [Mn(acac)$_2N_3$] has also been reported to be field dependent at low temperatures.[28]

The stronger coupling observed for the azide complex possibly reflects a more symmetrical orbital system in this group compared to the acetate derivative, assuming the pathway for exchange is a superexchange mechanism involving the π orbitals of the bridging group. The long Mn···Mn distance observed[7] in the acetate complex, 6.536 Å, would preclude a more direct pathway. The magnitude of exchange observed for [Mn(salen)N_3] is comparable to that observed in [Mn(acac)$_2N_3$] where the Mn···Mn distance is[12] 5.63 Å. The exchange coupling in [Mn(acen)N_3] is weaker than that observed in [Mn(acac)$_2N_3$] or [Mn(salen)N_3], which suggests there may also be an in-plane influence on J.

(iii) Dimers. The magnetic susceptibilities of both [Mn(salen)NCS] and [Mn(salen)Br] show quite sharp maxima at low temperatures (7 and 11 K, respectively), which are indicative of dimeric structural arrangements. In the absence of an X-ray

---

(26) Weng, C. H. Ph.D. Dissertation, Carnegie-Mellon University, Pittsburgh, PA, 1968.

(27) Hiller, W.; Strähle, J.; Datz, A.; Hanack, M.; Hatfield, W. E.; der Haar, L. W.; Gütlich, P. *J. Am. Chem. Soc.* **1984**, *106*, 329.

(28) Gregson, A. K.; Moxon, N. T. *Inorg. Chem.* **1982**, *21*, 586.

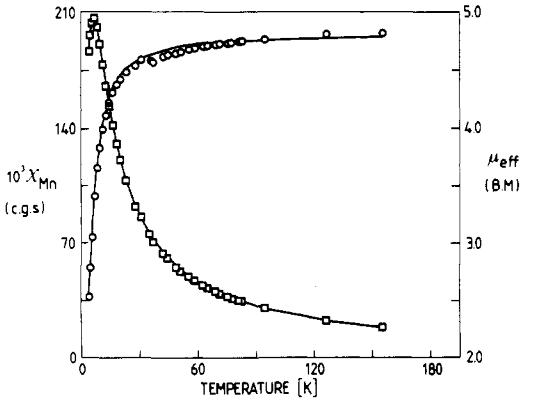

Figure 5. Temperature dependence of the magnetic moment (○) and molecular susceptibility (□) for a polycrystalline sample of [Mn(salen)SCN] (field 10 kG). Solid line is for $J = -0.44$ cm^{-1}, $D = -3.8$ cm^{-1}, and $g = 1.97$.

structure of either of these complexes, the exact molecular geometry is uncertain; however, it is probable that in both complexes Mn exists in an octahedral coordination with the anion and a phenolic oxygen of a neighboring [Mn(salen)] moiety making up the octahedron, as is observed in $[Fe(salen)Cl]_2$[29] and postulated in [Fe(salen)SCN].[20]

The infrared spectrum of [Mn(salen)SCN] shows bands attributable to the thiocyanate group at 2050 and 775 cm^{-1}, suggesting[31] coordination to the metal via nitrogen rather than the sulfur atoms. The preference of the Mn center for the nitrogen donor was also observed in the precursor molecule $[Mn(acac)_2SCN]_n$, which exists[11] as an infinite chain, where the Mn–S bond distance of 2.880 Å is very much longer than the corresponding Mn–N distance, 2.189 Å, even allowing for the larger covalent radius of sulfur. The presence of a second good donor atom, the phenolic oxygen, then results in the sulfur atom remaining uncoordinated.

The magnetic moment of [Mn(salen)NCS] drops slowly from 4.88 μ_B at 295 K to 4.80 μ_B at 120 K, and then more rapidly to 2.52 μ_B at 4.2 K (Figure 5). The susceptibility gradually increases as the temperature is lowered to 7 K, where it shows a sharp maximum. We initially attempted to fit the data to the simple $S = 2$ dimer coupled model.[3] The best fits obtained with this model placed the maximum in susceptibility at temperatures slightly greater than that observed, and χ_{calcd} was always greater than the observed value in the temperature region below 10 K, suggesting the need to include a ZFS term. Use of the more complete spin Hamiltonian model (eq 2) for a symmetrical dimer led to satisfactory fits over the entire temperature range, although it was not possible to distinguish the sign of D. As the complexes $[Mn(sal\text{-}N\text{-}R)_3]$ (R = Benz, Ph) and [Mn(salen)OAc] have negative D values, it is probable that a similar ground state will be present here. Careful variation of D and J then gave a best fit with $D = -3.8 \pm 0.2$ cm^{-1} and $J = -0.44 + 0.02$ cm^{-1} shown in Figure 5.

The magnetic moment of [Mn(salen)Br] shows a similar temperature dependence to the thiocyanate complex, dropping slowly from 4.7 μ_B at 300 K to 4.46 μ_B at 120 K and finally reaching 1.47 μ_B at 4.2 K. At all temperatures the susceptibility for this complex is less than that observed for the thiocyanate complex, implying a stronger exchange interaction. Fitting of the data to eq 2, with D assumed to be negative, confirmed this, and a best fit J value of -1.84 ± 0.10 cm^{-1} was deduced. As a result of the stronger coupling, the susceptibilities were found to be relatively insensitive to the size of the ZFS on the Mn(III) center with values between -0.6 and -1.3 cm^{-1} providing equally good fits.

The surprising difference in the strength of the coupling observed for the two binuclear complexes, which presumably have similar pathways for exchange, is thought to be a result of a greater delocalization of electrons about the anion in the thiocyanate complex, resulting in weaker exchange. This may also explain the larger zero-field splitting observed for this complex.

Conclusion

Powder susceptibility and magnetization measurements have shown that the zero-field splitting parameter, D, is negative in a series of monomeric Mn(III) Schiff-base complexes. Polycrystalline sample tend to act as oriented single crystals in the presence of magnetic fields unless the sample is mulled into a diamagnetic Vaseline paste. Magnetization measurements on these pastes show that D falls within the range -1.5 to -2.6 cm^{-1}, although the presence of weak magnetic exchange can result in a marked overestimation of the size of the ZFS if it is not taken into account.

Polymeric Mn(III) Schiff-base complexes are less susceptibile to such orientation effects, although complex magnetic behavior at low temperatures can result from the $M_S = \pm 2$ doublet lying lowest. The exact nature and strength of magnetic exchange in these complexes depend on both the anion and the in-plane Schiff base.

Acknowledgment. This work was supported by grants from the Australian Research Grants Scheme and Monash University Special Research Fund.

---

(29) Gerloch, M.; Mabbs, F. E. *J. Chem. Soc. A* **1967**, 1900.

(30) Gullotti, M.; Casella, L.; Pasini, A.; Ugo, R. *J. Chem. Soc., Dalton Trans.* **1977**, 339.

(31) Burmeister, J. L. *Coord. Chem. Rev.* **1968**, *3*, 225.

Contribution from the Department of Chemistry,
Monash University, Clayton, Victoria 3168, Australia

Magnetic Properties and Zero-Field Splitting in High-Spin Manganese(III) Complexes. 2. Axially Ligated Manganese(III) Porphyrin Complexes

BRENDAN J. KENNEDY and KEITH S. MURRAY*

Received June 11, 1984

Magnetization data in the temperature range 4.2–300 K and field range 5–50 kG for some five- and six-coordinate high-spin manganese(III) tetraaryl- and octaethylporphyrin complexes are reported. The results have been interpreted by means of spin Hamiltonian formalism that includes zero-field splitting and exchange terms. D values in the range -1 to -2.3 cm^{-1} and in some cases J values of less than -0.17 cm^{-1} were obtained. A brief discussion on the origin of the small, negative zero-field splitting in these and related complexes is given.

Introduction

This detailed study of the magnetic susceptibility and magnetization of Mn(III) porphyrin complexes complements a similar study on Mn(III) Schiff-base chelates described in part 1.[1] It also forms part of a wider study of paramagnetic susceptibilities in d-block metalloporphyrins,[2,3] a subject that until recently had been neglected in comparison to other physico-

---

[1] Kennedy, B. J.; Murray, K. S. *Inorg. Chem.*, preceding paper in this issue.